Materials Letters 368 (2024) 136705

Contents lists available at ScienceDirect

Materials Letters

journal homepage: www.elsevier.com/locate/matlet

Featured Letter

An EPR investigation on reduced Sn centres in $SrSnO_3$ perovskite

Adervando Silva [a], Franciska Hurdley [b], Andre Luiz Menezes de Oliveira [a], Thomas Slater [c], Ary da Silva Maia [a], Andrea Folli [b,*], Ieda Maria Garcia dos Santos [a,*]

[a] NPE-LACOM, Universidade Federal da Paraíba, João Pessoa-PB, 58051-085, Brazil
[b] Net Zero Innovation Institute, Cardiff Catalysis Institute, School of Chemistry, Cardiff University, Translational Research Hub, Cardiff, UK
[c] Cardiff Catalysis Institute, School of Chemistry, Cardiff University, Translational Research Hub, Cardiff, UK

ARTICLE INFO

Keywords:
Perovskite
Photocatalysis
Strontium stannate
Reduced species
Sn(III)

ABSTRACT

The use of the wide band gap $SrSnO_3$ semiconductor in photocatalysis has grown over the last few years, driven predominantly by sustainability given that its constituents are all Earth abundant elements. Using EPR spectroscopy, we elucidate the paramagnetic species present in the material, either intrinsic or photo-generated. EPR measurements confirmed the presence of paramagnetic oxygen vacancies (g = 2.0058) and a defect sensitive to visible light irradiation despite a wide optical band gap of 4.1 eV. This defect was confirmed to be Sn^{3+} (g = 2.014 and g = 1.994). Its concentration appears to increase with visible light irradiation, suggesting a photo-induced formation associated with electronic transitions from Sn^{2+} intra-band gap states to the conduction band.

1. Introduction

The use of photocatalysis has seen recent growth in different areas, including environmental remediation, hydrogen generation, sustainable fuels and chemicals production [1]. Different materials have been used for such applications, including $SrSnO_3$, which has also been used as dielectric materials, capacitors and sensors [2–4]. One advantage of $SrSnO_3$ is the absence of expensive rare metals and the large abundance of its elements. Despite this, little is known about the species involved during its photoactivation. In previous works [5–7], we observed that reduced species and structural disorder seem to have an important role in photocatalysis. In this letter, we endeavour on crystal defects and reduced centres exhibited by $SrSnO_3$ under irradiation.

2. Materials and methods

$SrSnO_3$ was synthesized by Pechini-modified method as described in our previous work [8] and calcined at 900 °C for 4 h. After calcination, $SrSnO_3$ was characterized using X-ray diffraction (XRD), UV–Vis absorption spectroscopy, Scanning transmission electron microscopy (STEM) and Electron paramagnetic resonance (EPR) spectroscopy. Details of the measurements are given in the Supplementary Information (SI).

3. Results and discussion

The XRD pattern of the $SrSnO_3$ (Fig. 1a) confirms the formation of the perovskite phase with orthorhombic *Pbnm*-type structure, according to ICDD 77–1798. The short-range symmetry was confirmed by Raman spectroscopy (Fig. S1a), which showed well-defined peaks, assigned to $SrSnO_3$. The presence of strontium carbonate ($SrCO_3$) was observed by Raman spectroscopy, IR spectroscopy (Fig. S1) and confirmed by STEM-EDX spectroscopy (Fig. S2), as usual for alkaline-earth perovskites obtained by the Pechini method. The UV–Vis absorption spectrum for $SrSnO_3$ (inset of Fig. 1a) displays a strong absorption in the UV region, with a direct band gap (E_g) value of 4.1 eV. A HAADF-STEM image is shown in Fig. 1b, with an extracted Fast Fourier Transform (Fig. 1c) displaying intensity peaks at values assigned to {1 1 2} and {0 2 0} planes, both with a spacing of approximately 2.8 Å for the structure calculated from the XRD pattern (a = 5.64 Å, b = 5.77 Å, c = 8.01 Å).

To elucidate electron/hole generation and trapping mechanisms under irradiation, we employed EPR spectroscopy. Paramagnetic species are present in the sample at all wavelengths the material is exposed to (Fig. 2), and even the spectrum in the dark shows the presence of paramagnetic species (spectrum ii, Fig. 3a). Interestingly, although Tauc plot analysis (Fig. 1a) revealed a wide band gap of 4.1 eV, suggesting that UV light is required for VB→CB electronic excitation and electron/hole formation; EPR spectroscopy (Fig. 2) indicates that the material is responsive to visible light, as evident by the EPR signal intensity that

* Corresponding authors.
E-mail addresses: follia@cardiff.ac.uk (A. Folli), ieda@quimica.ufpb.br (I.M.G. dos Santos).

https://doi.org/10.1016/j.matlet.2024.136705
Received 21 March 2024; Received in revised form 20 May 2024; Accepted 22 May 2024
Available online 23 May 2024

starts increasing between 510 nm and 480 nm, *i.e.*, at energies much lower than the expected 4.1 eV. This optical response cannot be attributed to VB→CB transitions, and it is an indication that intra-band gap donor or acceptor states are likely to be present.

To ascertain the chemical nature of these species and elucidate a picture of the $SrSnO_3$ band structure, further EPR analysis was conducted (Fig. 3), involving spectra recorded under irradiation at 455 nm, including kinetics after switching the light off; and after thermal reduction. The recorded EPR signal of $SrSnO_3$ is indicative of three clear resonances at $g = 2.014$, $g = 2.0058$ and $g = 1.994$, as well as a broad feature at lower magnetic induction. The EPR spectra match with previously observed isotropic resonances at g = 2.014 and g = 1.994, herein referred to as Sn_I^{3+} and Sn_{II}^{3+} respectively (Fig. 3c), indicating the presence of Sn^{3+} in two distinct crystallographic environments, as reported in Sn-based semiconductors such as $Sn_2P_2S_6$ [8], Sn oxide glasses [9], SnO_2 [10], ZnO:Sn [11], and Ca_2SnO_4:Al [12].

The isotropic nature of ***g*** for the S=½ Sn^{3+} is mostly dictated by the unpaired electron *s* orbital character. There are two stable magnetic isotopes of Sn with non-zero nuclear spin (^{117}Sn, ^{119}Sn). Both have a nuclear spin I=½ and occur in abundances of 7.68 % and 8.59 %, respectively. As a result, for each Sn^{3+} species, the resulting EPR spectrum consists of a central line (not exhibiting any hyperfine) and two low signal intensity doublets split by the hyperfine interaction. Due to the large magnitude of the hyperfine interaction (Table S1), the low-field doublet cannot be observed at X-band frequencies [13–15]. A high-field doublet has, in some cases, been reported (Table S1). The anticipated low signal intensity for this doublet (as depicted by the simulation of Sn_{II}^{3+} in Fig. 3c and based on a hyperfine interaction, which is an average of values reported in Table S1), coupled with the suboptimal signal-to-noise ratio of our spectrum at high magnetic induction

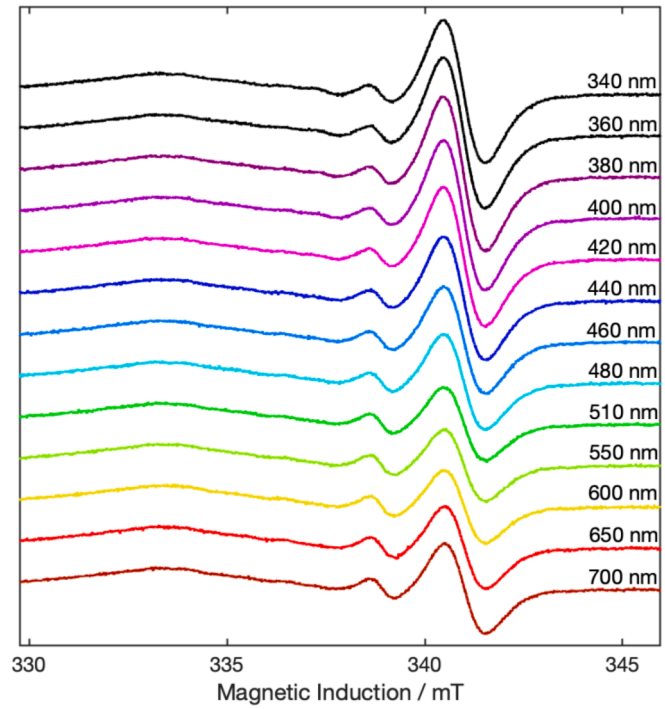

Fig. 2. X-band CW EPR spectra of untreated $SrSnO_3$ irradiated at different wavelengths.

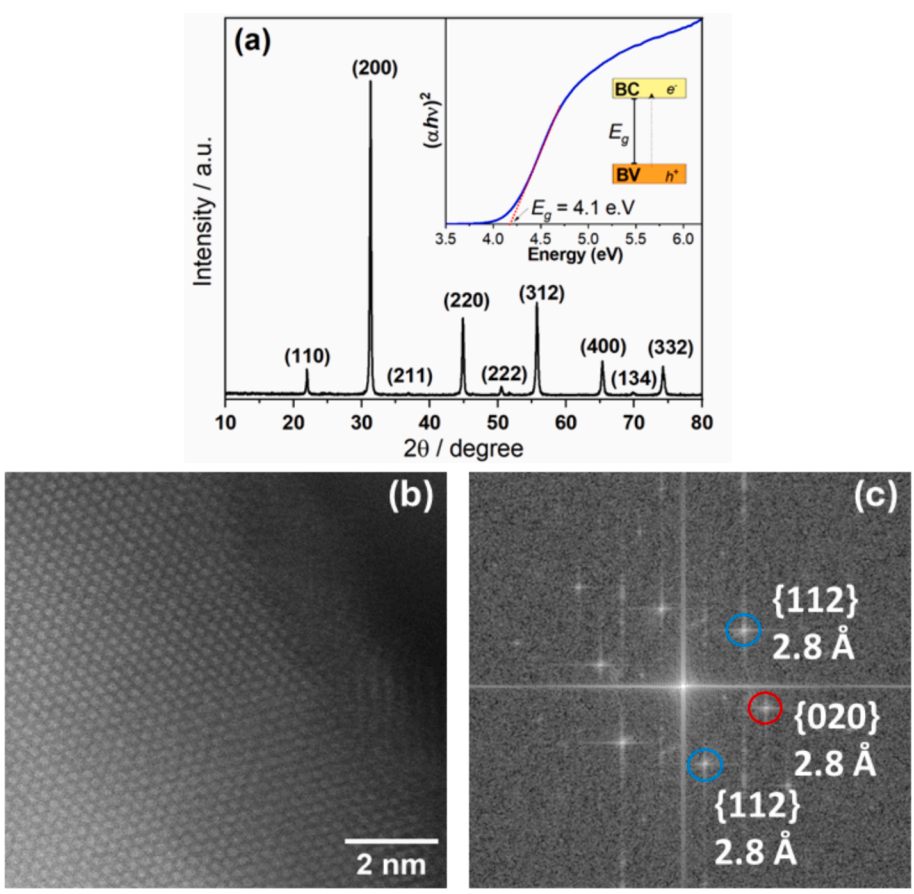

Fig. 1. Characterization of $SrSnO_3$ sample. (a) XRD pattern and UV–vis spectrum with E_g value (inset); (b) HAADF-STEM image of crystal oriented along ⟨201⟩ direction; (c) Cropped Fast Fourier Transform from the image displayed in (b).

(Fig. 3d), has most likely resulted in the doublet being overshadowed by the presence of noise in the spectrum. In addition, the detection of such hyperfine doublet for Sn_I^{3+} is even more problematic given the very low concentration of Sn_I^{3+} species (Fig. 3a-c) in the lattice. In Fig. 3a, a comparison of spectra ii. and iii. reveals that when exposed to 455 nm irradiation, the signal intensity of Sn_I^{3+} and Sn_{II}^{3+} species increases. This suggests that further Sn^{3+} may be formed upon irradiation with 2.7 eV photons. This light is not energetic enough to promote VB→CB transitions ($E_g = 4.1$ eV). Therefore, it appears evident that a donor intra-band gap state might be present. Considering that diamagnetic Sn^{2+} was previously detected in this material [5], its presence as intra-band gap donor state provides a reasonable explanation for the observed behaviour under blue-light irradiation.

The peak-to-peak signal intensity of the Sn_{II}^{3+} resonance was followed over time after light was turned off, with kinetics presented in Fig. 3e-f and described in the SI. The overall decay appears to occur at a very low rate, *i.e.*, 91 % of the total peak-to-peak EPR signal intensity after 30 min of irradiation is retained after 33.3 min from switching the light off, a further confirmation of the relatively high stability of Sn^{3+} species in $SrSnO_3$.

A considerably different behaviour was observed under the thermal reduction of $SrSnO_3$. The resonance at g = 2.0058 can be attributed to oxygen vacancies, which trap one electron and create a paramagnetic $V_O^{\bullet}$ species. This species did not respond to light stimuli as shown in Fig. 3a,

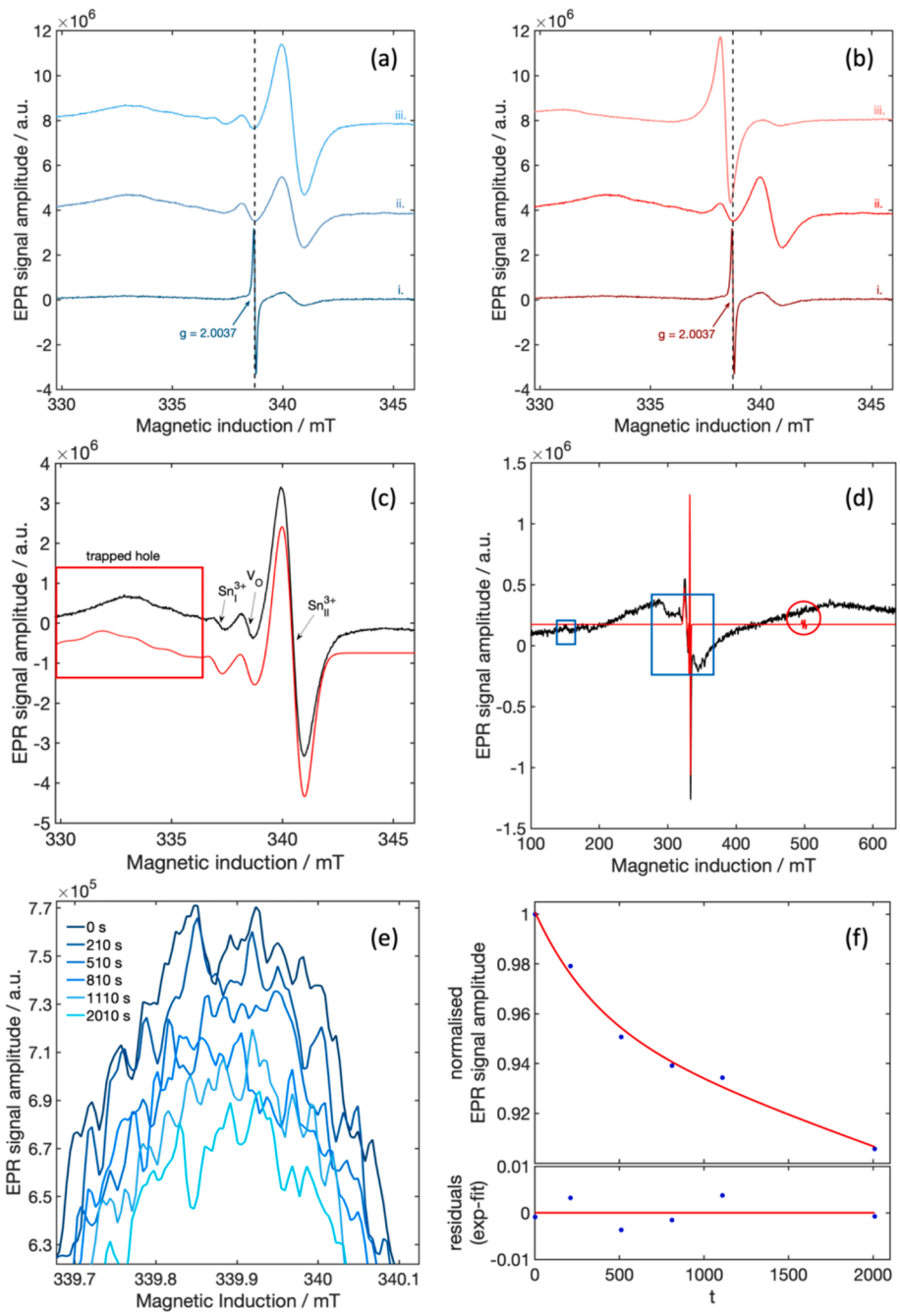

Fig. 3. X-band CW EPR spectra of $SrSnO_3$ measured at room temperature. (a) before (ii) and after (iii) 450 nm irradiation; (b) before (ii) and after (iii) reducing annealing; (c, d) experimental (black) and simulated (red) spectrum of a.ii (blue squares in figure (d) highlight resonances associated with Fe^{3+} impurities (not simulated) present in the sample); (e) maximum signal intensity of the Sn_{II}^{3+} species at regular time intervals after switching the 450 nm lamp off; (f) kinetics of Sn_{II}^{3+} EPR signal intensity after switching the lamp off. Spectra i in (a) and (b) refers to the internal standard (dpph).

but its EPR resonance signal intensity increased significantly after reducing annealing (Fig. 3b), in agreement with the assignation of the g = 2.0058 resonance to $V_O^{\bullet}$.

Finally, EPR spectra also revealed the presence of a much broader signal at 330 mT < B_0 < 336–337 mT (EPR resonance frequency 9.5 GHz). An unambiguous assignment to this broad resonance is challenging. Beside a contribution from Fe^{3+} impurities (Fig. 3d and [16]), the signal could arise from O^- centres (*i.e.* trapped valence band hole). A more exhaustive discussion on the latter can be found in [17,18].

The presented results hold significant importance in understanding Sn-based perovskite photocatalytic activity. The photocatalytic activity of this material has already been demonstrated with UV light . The generation of intra-band gap Sn^{3+} states following photo-sensitisation can also influence the overall kinetics of the photocatalytic process. In fact, interfacial single electron transfer to surface adsorbate (often the rate-determining-step in semiconductor photocatalysis [19]) occurs from a metal reduced state instead of directly from the conduction band [19].

4. Conclusions

Using EPR spectroscopy, Sn^{3+} paramagnetic centres in two different crystallographic environments are identified, for the first time, in $SrSnO_3$ perovskites. These centres exhibit a remarkable stability at room temperature. In addition, two other distinctive paramagnetic defects, *i.e.*, oxygen vacancies and, potentially, trapped holes, appears to be present in the $SrSnO_3$ perovskite. The concentration of Sn^{3+} centres can be augmented by irradiating the samples with visible light, in apparent contrast with the E_g = 4.1 eV; corresponding to the valence to conduction band transitions. This observation can be explained by the presence of an extrinsic optical band gap of 2.7 eV due to the presence of diamagnetic intra-band gap Sn^{2+} donor states which find confirmation in previous XPS studies.

CRediT authorship contribution statement

Adervando Silva: Writing – original draft, Methodology, Investigation, Data curation. **Franciska Hurdley:** Writing – original draft, Methodology, Investigation, Data curation. **Andre Luiz Menezes de Oliveira:** Writing – original draft, Methodology, Investigation, Data curation. **Thomas Slater:** Writing – original draft, Resources, Investigation. **Ary da Silva Maia:** Supervision, Methodology. **Andrea Folli:** Writing – original draft, Writing – review & editing, Methodology, Investigation, Data curation, Resources, Funding acquisition, Supervision, Project management. **Ieda Maria Garcia dos Santos:** Writing – original draft, Writing – review & editing, Methodology, Investigation, Data curation, Resources, Funding acquisition, Supervision, Project management.

Declaration of competing interest

The authors declare that they have no known competing financial interests or personal relationships that could have appeared to influence the work reported in this paper.

Data availability

Data will be made available on request.

Acknowledgements

The authors acknowledge Brazilian agencies CAPES/MEC (finance-code 001) and FAPESQ/PB (grant 1975/2022), Cardiff University Net Zero Innovation Institute and CCI Electron Microscopy Facility, part-funded by the European Regional Development Fund through the Welsh European Funding Office and The Wolfson Foundation, for financial support.

Appendix A. Supplementary data

Supplementary data to this article can be found online at https://doi.org/10.1016/j.matlet.2024.136705.

References

[1] C. Xu, Chem. Soc. Rev. 48 (2019) 3868–3902.
[2] L.M.C. Honorio, et al., Cerâmica 64 (2018) 559–569.
[3] Y. Pi, et al., Nano Energy 62 (2019) 861–868.
[4] I.A. de Sousa Filho, D.O. Freire, I.T. Weber, Environ. Sci. Pollut. Res. 28 (2021) 45009–45018.
[5] L.M.C. Honorio, et al., Appl. Surf. Sci. 528 (2020) 146991.
[6] L. Chantelle, Inorg. Chem. 59 (2020) 7666–7680.
[7] A.R.F.A. Teixeira, et al., J. Photochem. Photobiol. A Chem. 369 (2019) 181–188.
[8] A.T. Brant, et al., J. Phys. Condensed Matter 25 (2013) 205501.
[9] A.I. Aleksandrov, N.N. Bubnov, A.I. Prokofev, Appl. Magn. Reson. 9 (1995) 251–266.
[10] M. Ivanovskaya, E. Ovodok, V. Golovanov, Chem. Phys. 457 (2015) 98–105.
[11] A. Hausmann, P. Schreiber, Z. Physik 245 (1971) 184–190.
[12] G. Krieke, A. Antuzevics, B. Berzina, Mater. Today Commun. 28 (2021) 102592.
[13] I. Jaek, E. Realo, V. Seman, L. Mürk, Phys. Status Solidi 61 (1974) 745–755.
[14] N. Yamashita, S. Asano, J. Phys. C Solid State Phys. 9 (1976) L65–L67.
[15] Z. Egemberdiev, et al., Phys. Status Solidi 96 (1979) 867–875.
[16] T. Castner Jr., G. Newell, W. Holton, C. Slichter, J. Chem. Phys. 32 (1960) 668–673.
[17] R.F. Howe, M. Grätzel, J. Phys. Chem. 89 (1985) 4495–4499.
[18] C.A. Jenkins, D.M. Murphy, J. Phys. Chem. B 103 (1999) 1019–1026.
[19] M.R. Hoffmann, S.T. Martin, W. Choi, D.W. Bahnemann, Chem. Rev. 95 (1995) 69–96.